Electronic Supplementary Material (ESI) for Journal of Materials Chemistry A.
This journal is © The Royal Society of Chemistry 2015

Supporting information

3D Hierarchical Porous Zinc-Nickel-Cobalt Oxides Nanosheets Grown on Ni Foam as Binder-Free Electrodes for Electrochemical Energy Storage

Huixin Chen [a, 1], Qiaobao Zhang [b, d, 1], Xiang Han [c], Junjie Cai [b], Meilin Liu [d], Yong Yang [a, *], Kaili Zhang [b, *]

[a] State Key Laboratory for Physical Chemistry of Solid Surfaces, Department of Chemistry, Xiamen University, Xiamen, 361005, P. R. China

[b] Department of Mechanical and Biomedical Engineering, City University of Hong Kong, 83 Tat Chee Avenue, Kowloon, Hong Kong

[c] Semiconductor Photonics Research Center, Department of Physics, Xiamen University, Xiamen, 361005, P. R. China

[d] School of Materials Science and Engineering, Georgia Institute of Technology, 771 Ferst Drive, Atlanta 30332-0245, GA, United States

[1] These authors contributed equally to this work

[*]Corresponding authors:

Yong Yang, E-mail address: yyang@xmu.edu.cn

Kaili Zhang, E-mail address: kaizhang@cityu.edu.hk

The crystal phase of the as-synthesized ZNCO-precursor nanosheets on Ni foam was determined by X-ray diffraction (XRD) with the result shown in Figure S1. Besides from the three strong peaks from Ni foam substrate, all the identified peaks can be assigned to pure orthorhombic cobalt carbonate hydroxide (PDF#48-0083), indicating that the Ni and Zn co-incorporated in the host layer of cobalt carbonate hydroxide to form ZNCO carbonate hydroxides has no effect on the crystal structure of cobalt carbonate hydroxide.

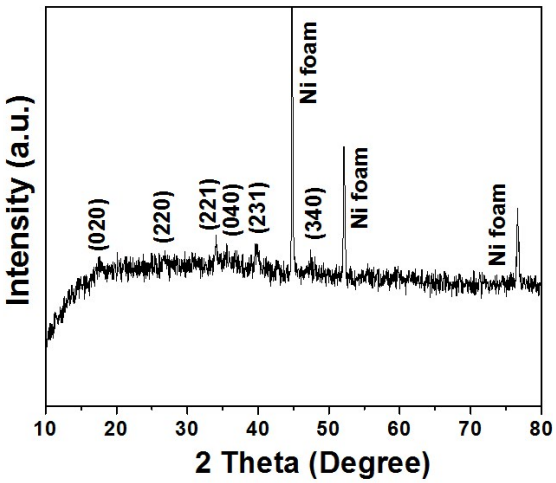

Figure S1 XRD pattern of ZNCO-precursor nanosheets on Ni foam.

Table S1 ICP-MS results of Ni/Zn/Co molar ratio of ZNCO nanosheets

Element	Mas concentration (ug/mL)	Molar concentration (umol/mL)
Ni	11.3	0.193
Zn	12.8	0.196
Co	24.9	0.42

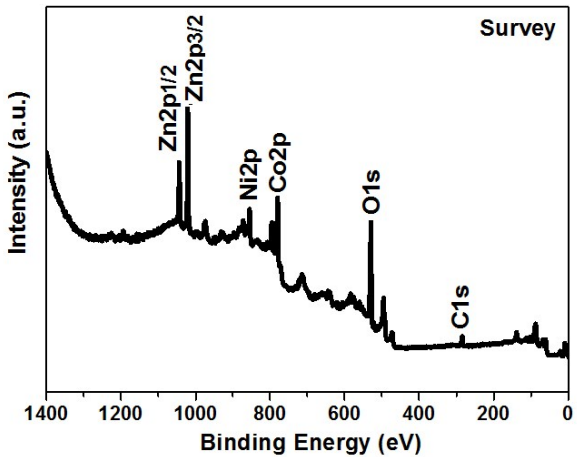

Figure S2 XPS survey spectrum of ZNCO nanosheets.

The ZNCO nanosheets powder was obtained by thermally converted from their corresponding ZNCO-precursor nanosheets, which were collected from the precipitates at the bottom of beaker resulted from the reacted solution by centrifugation. Figure S3 shows the SEM images of off-substrate ZNCO nanosheets. From Figure S3(a-b), we can see that they show a flower-like shape composed of interconnected ultrathin nanosheets with enough space between each other. Figure S3(c) and (d) shows the typical discharge-charge voltage profiles for the first, second, third and 50th cycles and cycle performance of ZNCO nanosheets pasted electrode at a current density of 0.1 Ag^{-1}, respectively. As shown in Figure S3(d), the ZNCO nanosheets pasted electrode demonstrates bad cycling performance with the capacity faded very quickly from the first cycle. This may due to a fact that a pasted electrode cannot ensure the direct contact of the active material with the current collector or preserve the quality of the adhesion if the binder and conductive additive are subjected to cyclical changes in the volume, stress, and strain of the active material. The randomness in the arrangement of the hierarchical structures also increased the diffusion lengths for electrons and Li^{+}. Additionally, the presence of binder could also

impede electron conduction between the active material and the current collector because most binders with good adhesion properties are electron insulators.

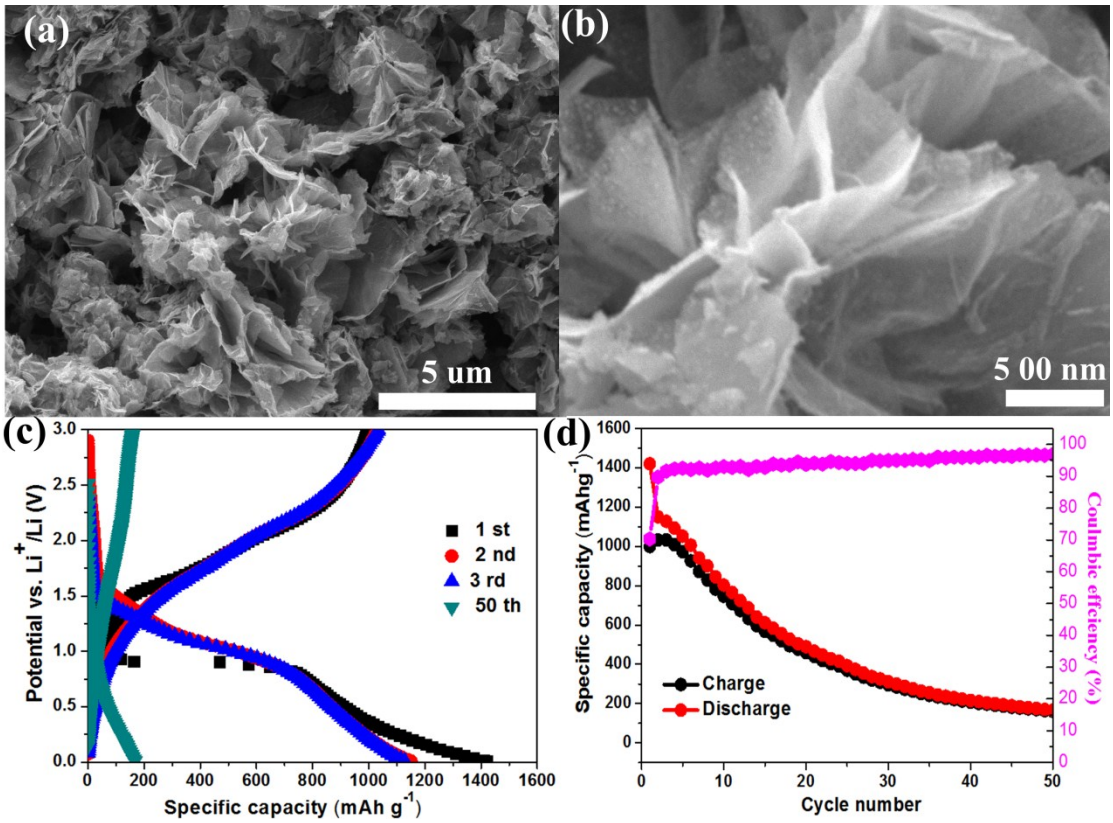

Figure S3 (a-b) SEM images of off-substrate ZNCO nanosheets, (c) typical discharge-charge voltage profiles for the first, second, third and 50th cycles and (d) cycling peformanance of ZNCO nanosheets pasted electrode at current density of 0.1 Ag^{-1}.

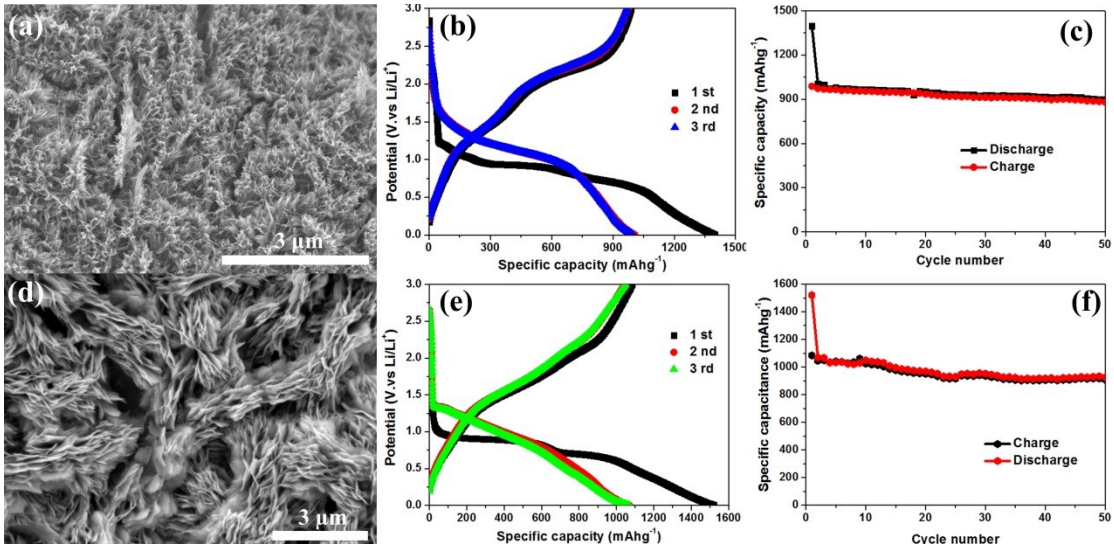

Figure S4. (a) SEM image of $NiCo_2O_4$ (NCO) nanosheets on Ni foam, (b) Discharge/charge profiles of as-prepared NCO nanosheets electrodes in the 1st, 2 nd and 3 rd cycles at a constant current of 200 mAg^{-1} and (c) its corresponding cycling performance at current density of 200 mAg^{-1}, (d) SEM image of $ZnCo_2O_4$ (ZCO) nanosheets on Ni foam, (e) Discharge/charge profiles of as-prepared ZCO nanosheets electrodes in the 1st, 2 nd and 3 rd cycles at a constant current of 200 mAg^{-1} and (f) its corresponding cycling performance at current density of 200 mAg^{-1}.

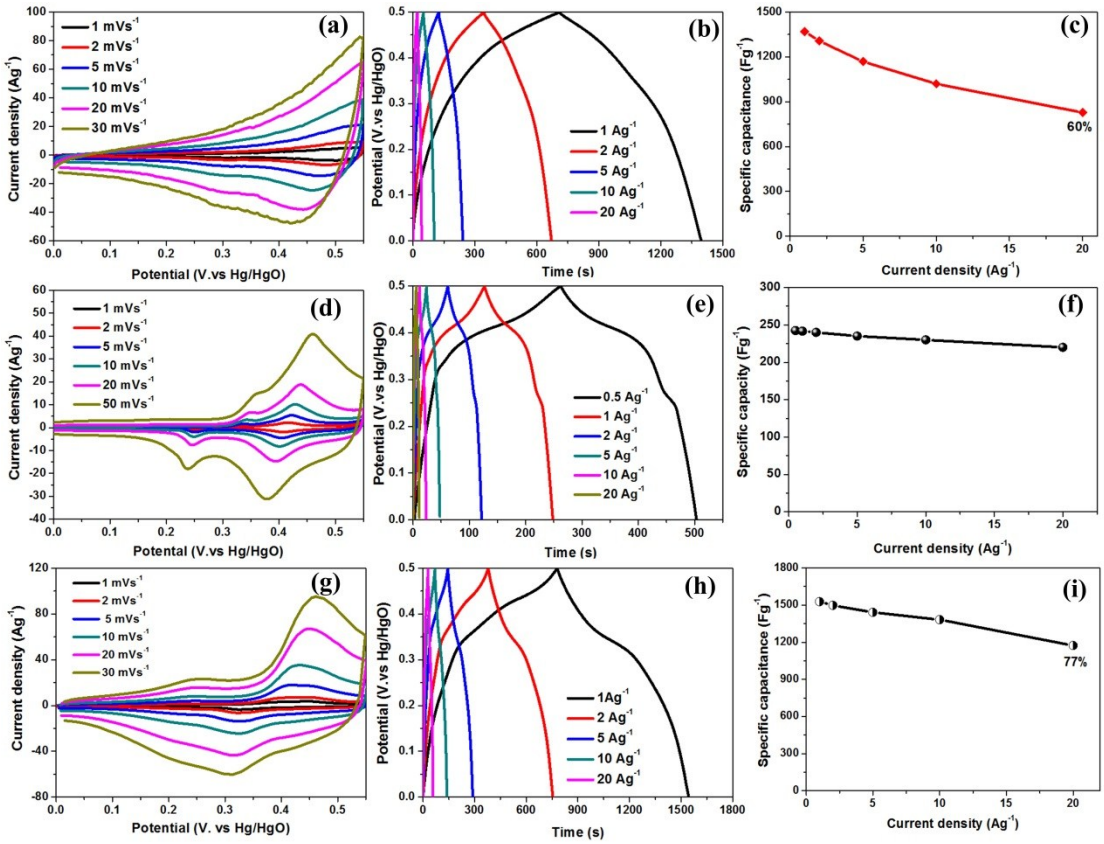

Figure S5. (a) CV curves of the ZCO/Ni foam electrode at various scan rates ranging from 1 to 30 mVs^{-1}, (b) charge–discharge curves of ZCO/Ni foam electrode at various current densities, and (c) the corresponding capacitance of ZCO/Ni foam electrode as a function of current density, (d) CV curves of the CO/Ni foam electrode at various scan rates ranging from 1 to 50 mVs^{-1}, (e) charge–discharge curves of CO/Ni foam electrode electrode at various current densities, and (f) the corresponding capacitance of CO/Ni foam electrode as a function of current density, (g) CV curves of the NCO/Ni foam electrode at various scan rates ranging from 1 to 30 mVs^{-1}, (h) charge–discharge curves of NCO/Ni foam electrode at various current densities, and (i) the corresponding capacitance of NCO/Ni foam electrode as a function of current density

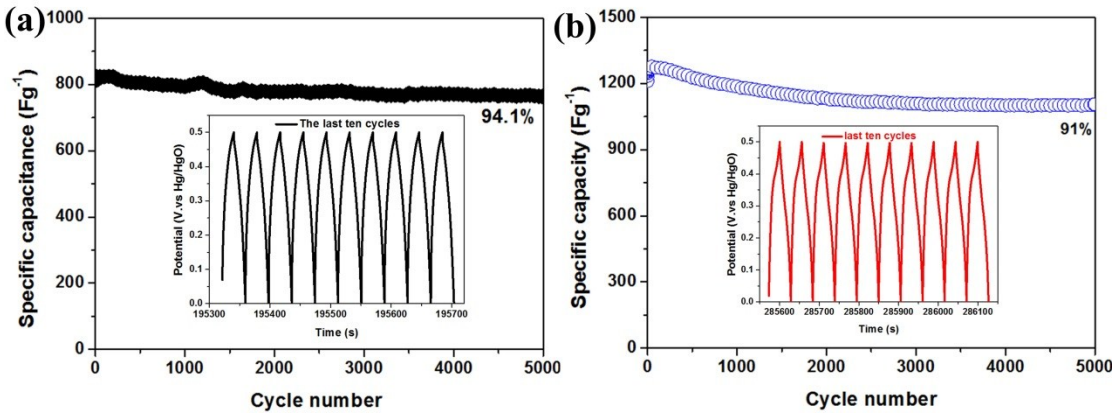

Figure S6. Cycling performance of the (a) ZCO nanosheets/Ni foam and (b) NCO nanosheets/Ni foam electrode at current density of 20 Ag^{-1} for 5000 cycles, inset is their corresponding charge/ discharge curves of the last ten cycles for the 5000 cycles.

Table S2 Comparison of electrochemical properties as the anode materials for LIBs between various other TMOs binder-free electrodes reported in the literature and ZNCO nanosheets/Ni foam electrode in this work.

Other TMOs anodes	Charge capacity ($mAhg^{-1}$)	Voltage range(V)	Current density (mAg^{-1})	References
Nanorod-assembled Co_3O_4 hexapods/Cu foil	800 (after 40cycles)	0.01–3.0	100	[1]
Co_3O_4 nanosheets/Ni foam	631 (after 50 cycles)	0.01−3.0	150	[2]
Leaf-like $ZnCo_2O_4$/Ni foam	1040 (after 60 cycles)	0.01–3.0	100	[3]
Flower-like $ZnCo_2O_4$ nanowires/carbon cotton	900 (after50cycles)	0.01-3.0	200	[4]
$NiCo_2O_4$ nanosheet/ Reduced Graphene Oxide	954 (after 50 cycles)	0.01-3.0	200	[5]
$NiCo_2O_4$/graphene nanosheets/Ni foam	1031 (after 20 cycles)	0.01- 3.0	150	[6]
NiO nanoflake arrays/Cu foil	720 (after 20 cycles)	0.01-3.0	100	[7]
ZNCO nanosheets/Ni foam	1130 (after 50 cycles) 663 (after 1000 cycles)	0.01-3.0	200 1000	This work

Table 3 Comparison of electrochemical properties as electrode materials for SCs between various other ZCO, NCO and CO binder-free electrodes reported in the literature and ZNCO nanosheets/Ni foam electrode in this work.

Electrode materials	Capacitance	Capacitance retention	Refs
Flowerlike ZCO microspheres/Ni foam	684.9 Fg^{-1} at $1Ag^{-1}$ 336.6 Fg^{-1} at 15 Ag^{-1}	49% from $1Ag^{-1}$ to $15Ag^{-1}$	8
Flower-like NCO/ 3D graphene foam	1402 Fg^{-1} at $1Ag^{-1}$ 1080 Fg^{-1} at 20 Ag^{-1}	77% from $1Ag^{-1}$ to $20Ag^{-1}$	9
CO nanowires/Ni foam	1160 Fg^{-1} at $2Ag^{-1}$ 820 Fg^{-1} at 20 Ag^{-1}	70% from $2Ag^{-1}$ to $20Ag^{-1}$	10
ZCO nanorods/Ni foam	1400 Fg^{-1} at $1Ag^{-1}$ 1015 Fg^{-1} at 20 Ag^{-1}	72.5 % from $1Ag^{-1}$ to$20Ag^{-1}$	11
NCO nanoneedles/3D graphene/Ni foam	1588 Fg^{-1} at $1Ag^{-1}$ 976 Fg^{-1} at 20 Ag^{-1}	61% from $1Ag^{-1}$ to $20Ag^{-1}$	12
NCO nanowires/carbon textiles	1283 Fg^{-1} at $1Ag^{-1}$ 1010 Fg^{-1} at 20 Ag^{-1}	79% from $1Ag^{-1}$ to $20Ag^{-1}$	13
ZCO nanoflakes/Ni foam	1220 Fg^{-1} at $2Ag^{-1}$ 881 Fg^{-1} at 10 Ag^{-1}	72% from 2 Ag^{-1} to 10 Ag^{-1}	14
ZNCO nanosheets/Ni foam	1728 Fg^{-1} at $1Ag^{-1}$ 1512 Fg^{-1} at 20 Ag^{-1}	87.5% from $1Ag^{-1}$ to $20Ag^{-1}$	**This work**

CO:Co_3O_4, NCO: $NiCo_2O_4$, ZCO: $ZnCo_2O_4$, ZNCO: $Zn_{0.75}Ni_{0.75}Co_{1.5}O_4$

References

1. L. Wang, B. Liu, S. Ran, H. Huang, X. Wang, B. Liang, D. Chen, and G. Shen, *J. Mater. Chem.*, 2012, **22**, 23541.

2. Y. Fan, H. Shao, J. Wang, L. Liu, J. Zhang, and C. Cao, *Chem. Commun. (Camb).*, 2011, **47**, 3469–71.

3. H. Long, T. Shi, S. Jiang, S. Xi, R. Chen, S. Liu, G. Liao, and Z. Tang, *J. Mater. Chem. A*, 2014, **2**, 3741.

4. S. G. Mohamed, T.-F. Hung, C.-J. Chen, C. K. Chen, S.-F. Hu, R.-S. Liu, K.-C. Wang, X.-K. Xing, H.-M. Liu, A.-S. Liu, M.-H. Hsieh, and B.-J. Lee, *RSC Adv.*, 2013, **3**, 20143.

5. G. Gao, H. Bin Wu, and X. W. D. Lou, *Adv. Energy Mater.*, 2014, DOI:10.1002/aenm.201400422.

6. Y. Chen, J. Zhu, B. Qu, B. Lu, and Z. Xu, *Nano Energy*, 2014, **3**, 88–94.

7. H. Wu, M. Xu, H. Wu, J. Xu, Y. Wang, Z. Peng, and G. Zheng, *J. Mater. Chem.*, 2012, **22**, 19821.

8. W. Fu, X. Li, C. Zhao, Y. Liu, P. Zhang, J. Zhou, X. Pan, and E. Xie, *Mater. Lett.*, 2015, **149**, 1–4.

9. C. Zhang, T. Kuila, N. H. Kim, S. H. Lee, and J. H. Lee, *Carbon N. Y.*, 2015, **89**, 328–339.

10. F. Zhang, C. Yuan, X. Lu, L. Zhang, Q. Che, and X. Zhang, *J. Power Sources*, 2012, **203**, 250–256.

11. B. Liu, B. Liu, Q. Wang, X. Wang, Q. Xiang, D. Chen, and G. Shen, *ACS Appl. Mater. Interfaces*, 2013, **5**, 10011–10017.

12. D. Cai, S. Xiao, D. Wang, B. Liu, L. Wang, Y. Liu, H. Li, Y. Wang, Q. Li, and T. Wang, *Electrochim. Acta*, 2014, **142**, 118–124.

13. L. Shen, Q. Che, H. Li, and X. Zhang, *Adv. Funct. Mater.*, 2013, DOI: 10.1002/adfm.201303138.

14. J. Cheng, Y. Lu, K. Qiu, H. Yan, X. Hou, J. Xu, L. Han, X. Liu, J.-K. Kim, and Y. Luo, *Phys. Chem. Chem. Phys.*, 2015, **17**, 17016–17022.